HAL
archives-ouvertes.fr

Amphiregulin promotes resistance to gefitinib in nonsmall cell lung cancer cells by regulating Ku70 acetylation.

Benoît Busser, Lucie Sancey, Véronique Josserand, Carole Niang, Saadi Khochbin, Marie Favrot, Jean-Luc Coll, Amandine Hurbin

▶ **To cite this version:**

Benoît Busser, Lucie Sancey, Véronique Josserand, Carole Niang, Saadi Khochbin, et al.. Amphiregulin promotes resistance to gefitinib in nonsmall cell lung cancer cells by regulating Ku70 acetylation.. Molecular Therapy, Nature Publishing Group, 2010, 18 (3), pp.536-43. 10.1038/mt.2009.227 . inserm-00425467

HAL Id: inserm-00425467
https://www.hal.inserm.fr/inserm-00425467

Submitted on 21 Oct 2009

HAL is a multi-disciplinary open access archive for the deposit and dissemination of scientific research documents, whether they are published or not. The documents may come from teaching and research institutions in France or abroad, or from public or private research centers.

L'archive ouverte pluridisciplinaire **HAL**, est destinée au dépôt et à la diffusion de documents scientifiques de niveau recherche, publiés ou non, émanant des établissements d'enseignement et de recherche français ou étrangers, des laboratoires publics ou privés.

Amphiregulin promotes resistance to gefitinib in Non-Small Cell Lung Cancer cells by regulating Ku70 acetylation

Benoît BUSSER[1,2,3], Lucie SANCEY[1,2], Véronique JOSSERAND[1,2], Carole NIANG[1,2], Saadi KHOCHBIN[1,2], Marie C FAVROT[1,2,3], Jean-Luc COLL[1,2] and Amandine HURBIN[1,2]

[1] INSERM, U823, Institut Albert Bonniot, Grenoble, F-38042, France. [2] Université Joseph Fourier, Grenoble, F-38042, France. [3] CHRU Grenoble, Hôpital Michallon, UF Cancérologie Biologique et Biothérapie, Grenoble, F-38000, France.

Correspondence should be addressed to: Amandine Hurbin or Jean-Luc Coll

INSERM U823, Institut Albert Bonniot, BP170 Grenoble, F-38042 cedex 9, France.

Phone: 33-4-76-54-95-53; Fax: 33-4-76-54-94-13

E-mail: amandine.hurbin@ujf-grenoble.fr

Short title: Ku70 acetylation and gefitinib resistance

Abstract

Multiple molecular resistance mechanisms reduce the efficiency of receptor tyrosine kinase inhibitors such as gefitinib in Non-Small Cell Lung Cancer. We previously demonstrated that amphiregulin inhibits gefitinib-induced apoptosis in Non-Small Cell Lung Cancer cells by inactivating the proapoptotic protein BAX. In this part of the investigation, we studied the molecular mechanisms leading to BAX inactivation. We show that amphiregulin prevents gefitinib-mediated acetylation of Ku70. This augments the BAX-Ku70 interaction and therefore prevents BAX-mediated apoptosis. Accordingly, amphiregulin or Ku70 knock down restore BAX activation and apoptosis in gefitinib-treated H358 cells *in vitro*. In addition, overexpression of the histone acetyltransferase CBP or treatments with histone deacetylase inhibitors sensitize H358 cells to gefitinib. Moreover, a treatment vorinostat, a histone deacetylase inhibitor strongly sensitized tumors to gefitinib *in vivo*. These findings suggest new prospects in combining both histone deacetylase and Epidermal Growth Factor Receptor inhibitors for the treatment of Non-Small Cell Lung Cancer.

Introduction

EGFR is frequently overexpressed in non-small cell lung cancers (NSCLC) and correlates with a poor clinical outcome [1, 2]. Inhibitors of the tyrosine kinase activity of EGFR (the EGFR-TKI family) were therefore developed. Small molecules that block the ATP binding site of the cytoplasmic domain of EGFR, such as gefitinib or erlotinib, showed potent antitumor activity against previously treated NSCLC [3, 4]. However, the limited response rates of patients to EGFR-TKI [5] led to investigating the mechanisms leading to resistance to EGFR-TKI treatments.

The level of expression of the EGFR ligand amphiregulin (Areg) was correlated with a poor response to gefitinib [6]. Areg is associated with shortened survival of patients with NSCLC and poor prognosis [7]. Our group previously reported that Areg inactivates the pro-apoptotic protein BAX [8] and inhibits gefitinib-induced apoptosis in NSCLC (see suppl. file S1). However, the molecular mechanisms governing Areg- and gefitinib-mediated BAX inactivation in NSCLC cells are still unknown.

Following its activation, BAX translocates from the cytosol to the outer mitochondrial membrane where it oligomerizes, rendering the membrane permeable, and allowing the release of several mitochondrial death-promoting factors [9]. The Ku70 DNA end-joining protein has recently been shown to suppress apoptosis by sequestering BAX from the mitochondria [10, 11]. In contrast, when Ku70 is acetylated, it releases BAX, allowing it to translocate to the mitochondria and trigger cytochrome c release, leading to caspase-dependent death. Ku70 was first characterized as part of the Ku70/Ku80 heterodimer that is essential for the repair of DNA double-strand breaks by nonhomologous end joining (NHEJ) and the rearrangement of antibody and T cell receptor genes via V(D)J recombination [12],

telomere maintenance and transcriptional regulation [13]. Ku70 activity could be determined by its acetylation status, like other nonhistone proteins such as p53 and Hsp90 [14]. The acetylation level is regulated by both histone acetyltransferase (HAT) and histone deacetylase (HDAC) activities. Recent reports suggest that there is a positive relationship between Ku70 and the development of cancer, presenting Ku70 as an important target for anticancer drug development [11].

In this study, we investigated the role of Ku70 in the Areg-regulated activity of gefitinib. We show that Areg inhibits apoptosis normally induced by gefitinib by an acetylation-dependent pathway leading to BAX inactivation. Areg reduces the acetylation of the protein Ku70, and thus enhances BAX inactivation. Consequently, enhancing acetylation abolishes the protective effect of Areg and renders NSCLC cells more sensitive to gefitinib treatment *in vitro* and *in vivo*.

Results

Areg and Ku70 inhibit gefitinib-induced apoptosis in H358 NSCLC cells.

H358 NSCLC cells overexpress Areg [15]. Transfection of H358 cells with anti-Areg small interfering RNAs (Areg siRNAs) strongly reduced the secreted levels of Areg, as compared to control siRNAs, 3 and 4 days after transfection (Fig. 1a). In addition, as shown in Fig. 1b, Ku70 siRNA transfection considerably silenced the endogenous Ku70 in H358 cells. Interestingly, while anti-Areg or anti-Ku70 siRNA transfection did not induce apoptosis, it significantly sensitized H358 cells to 0.5 μM gefitinib (Fig. 1c), suggesting that both Areg and Ku70 can reduce gefitinib efficiency. In addition, we verified that the Ku70 expression

level was not modified by gefitinib and/or Areg treatments in the H358 cell line (data not shown). This indicated that Ku70 protein levels did not fluctuate with the Areg/gefitinib cross-talk.

Areg and Ku70 inhibit BAX conformational change.

We then investigated the relationship between gefitinib activity, Areg, Ku70 and BAX activation in H358 cells. We analyzed BAX activation by flow cytometry using an antibody that recognizes the exposed N-terminus extremity of activated BAX but not the protein in its inactive conformation [16]. The intensity of BAX immunostaining (Fig. 2a, upper panel) as well as the percentage of positively stained cells (Fig. 2b) were not modified by the gefitinib treatment, showing that BAX is not activated in these conditions. In addition, Areg or Ku70 knock down had a limited influence on BAX activation, since the exposure of its N-terminus moiety was not modified. In sharp contrast, co-treatment of the cells by Areg siRNAs (Fig. 2a middle panel and Fig. 2b) or Ku70 siRNAs (Fig. 2a lower panel and Fig. 2b) and gefitinib was associated with an activation of BAX. These data suggested that both Areg and Ku70 prevent BAX conformational activation, therefore inhibiting gefitinib activity.

Areg increases BAX/Ku70 interaction.

To further demonstrate the role of Ku70 on Areg-dependent BAX inactivation, we measured the interaction between BAX and Ku70 using coimmunoprecipitation assays. We observed a low basal interaction between BAX and Ku70 in control H358 cells (Fig. 3a), which was enhanced under gefitinib treatment but only in the presence of Areg. Areg knock down significantly prevented this increase. This suggests that the Areg survival factor could limit gefitinib toxicity by increasing BAX/Ku70 aggregate formation.

This hypothesis is sustained by our results with another NSCLC cell line H322, which does not secrete Areg [15]. We showed that in H322, BAX/Ku70 interaction was not enhanced in the presence of gefitinib (Fig. 3b). Adjunction of recombinant Areg in the culture medium slightly, but reproducibly, increased the sequestration of BAX by Ku70.

Areg inhibits the acetylation of Ku70.

The interaction between BAX and Ku70 is regulated by acetylation. To further assess the effect of Areg on the state of Ku70 acetylation, we immunoprecipitated cytoplasmic Ku70 in H358 cells. After a treatment with gefitinib, the acetylation level of cytoplasmic Ku70 was below detection levels in our control conditions (Fig. 3c, left panel). However and as previously observed in figure 3a, the gefitinib treatment enhanced the interaction between BAX and Ku70. This was demonstrated after reprobing the same blot with the anti-BAX antibody (bottom panel). In contrast, acetylation of Ku70 was markedly increased and detectable when H358 cells were treated with gefitinib and anti-Areg siRNAs (upper panel). As expected, this hyperacetylation of Ku70 prevented BAX-Ku70 interaction, since we observed no detectable signal after BAX immunostaining (bottom panel). These results provide strong evidence that Areg inhibits the gefitinib-mediated acetylation of Ku70 and therefore enhances the sequestration of BAX by Ku70.

Ku70 acetylation increases the sensitivity of NSCLC cells to gefitinib

In vivo acetylation of proteins results from a subtle equilibrium between the opposite activities of acetyltransferases and deacetylases. Ku70 is known to be acetylated by HAT such as CBP, p300 and PCAF, whereas it can be deacetylated by both classes I/II HDAC and class III/sirtuin deacetylases [10]. To assess the involvement of acetylation, we first examined gefitinib-induced apoptosis in H358 cells overexpressing CBP. Overexpression of CBP had

no significant effect per se, but sharply increased the amount of apoptosis in gefitinib-treated H358 cells as compared to control-transfected cells (Fig. 4a).

H358 cells were then treated with several HDAC inhibitors. While concentrations of up to 200 ng/ml trichostatin A (TSA, classes I/II HDAC inhibitor) alone did not significantly induce apoptosis, its combination with gefitinib showed a very significant and dose-dependent induction of apoptosis (Fig. 4b). Gefitinib, in the presence of 200 ng/ml TSA, was ten times more toxic than when used alone. Similarly, suberoylanilide hydroxamic acid (SAHA or vorinostat, classes I/II HDAC inhibitor, Fig. 4c) or nicotinamide (NAM, class III/sirtuin deacetylases inhibitor, Fig. 4d) increased gefitinib-induced apoptosis. There was no significant effect of vorinostat or NAM alone. These results suggest that an increased acetylation by HAT overexpression or HDAC inhibition sensitizes the cells to gefitinib.

TSA increases the gefitinib-mediated acetylation of Ku70.

We then investigated whether increasing acetylation affected the gefitinib-mediated BAX-Ku70 interaction. The effect of TSA on cytoplasmic Ku70 was studied. TSA increased the acetylation of cytoplasmic Ku70 in gefitinib-treated cells (Fig. 5a, upper panel). As expected, this increased acetylation of Ku70 was associated with a reduction of the BAX-Ku70 interaction (Fig. 5a, middle panel). These results suggested that TSA sensitizes the cells to gefitinib's effect by enhancing Ku70 acetylation, leading to the subsequent release of BAX.

To consolidate this result, we constructed a K539R/K542R Ku70 mutant. Both lysines are known targets for acetylation, and govern BAX binding to Ku70. Their substitution by arginine amino acids prevents Ku70 acetylation [10, 17, 18]. A control (empty plasmid), or plasmids encoding for wild-type or Ku70 mutant proteins, were co-transfected in H358 cells and the level of apoptosis in the transfected cells was measured. As expected, 0.5 µM gefitinib or 200 ng/ml TSA alone did not induce significant apoptosis in any of the transfected

cells (Fig. 5b). The combined gefitinib and TSA treatments induced 50% apoptosis in control- or Ku70 wild-type-transfected cells, whereas only 30% of the cells transfected with the mutant form of Ku70 were apoptotic ($p < 0.05$) (Fig. 5b). This experiment demonstrated that both lysines 539 and 542, necessary to the BAX-Ku70 interaction and Ku70 acetylation [17], are crucial for apoptosis induced by gefitinib and TSA co-treatment.

Antitumor efficacy of dual targeting HDAC and EGFR *in vivo*

Results presented in figures 4 and 5 suggest that HDAC inhibitors counteract the protective effect of Areg and sensitize cells to gefitinib. To determine whether HDAC inhibitors are able to enhance the antitumor activity of gefitinib *in vivo*, we tested the effects of gefitinib, vorinostat, and their combination on the growth of H358 NSCLC xenograft tumors established in nude mice. Mice treated with a low concentration of gefitinib or vorinostat alone did not show reduced tumor growth as compared to control mice (Fig. 6a). Mice treated with gefitinib and vorinostat combination treatment showed a strong inhibition of tumor growth as compared to control mice or to mice treated with gefitinib or vorinostat alone (Table 1). At the end of the study, the mean tumor volume in the combined-treatment group was 36% ($p < 0.01$) of the mean volume in the control group. No major modification on the level of acetylation under vorinostat treatment was observed using an anti-acetylated histone H3K9 antibody or an anti-acetylated proteins antibody on total proteins extracts and western blot analysis (data not shown) or after immunolabeling of tumor sections at the end of this experiment (Fig 6b, upper panel). In tumors from control mice or from mice treated with vorinostat or gefitinib alone, more than 40% of tumor cells are actively proliferating and thus expressed elevated levels of the Ki67 nuclear protein, whereas only 16% of the cells were cycling in the combined-treatment group (p 0.0039, Fig 6b, lower panel and histogram). Gefitinib, vorinostat or the combination of both treatments were associated with increased

levels of cleaved-caspase-3 in the tumors (Fig 6c). These findings suggest that the combined treatment enhanced the antitumor activity of each drug *in vivo* by reducing the proliferation of tumor cells. The combination of both molecules does not increase the level of apoptosis observed with each treatment separately. Taken together, these results indicate that the antitumor activity of gefitinib is enhanced when vorinostat is also present.

Discussion

In the presence of Areg, NSCLC cells resist apoptosis induced by EGFR-TKI treatment such as gefitinib through BAX inactivation (see suppl. file S1). In this study, we demonstrate that this effect is due to an acetylation-dependent mechanism leading to BAX sequestration by Ku70. We suggest a therapeutic approach to restore the EGFR-TKI sensitivity *in vitro* and *in vivo*.

We previously established that Areg inhibits BAX conformational activation and thus its translocation from the cytosol to the mitochondria in NSCLC cells [8]. Several groups have shown the involvement of Ku70 in BAX inactivation in various pathologies such as neuroblastoma [17], leukemic cells [19], genotoxic stress response [20] or imatinib resistance [21, 22]. Here, we demonstrate that Ku70 binds to and inhibits BAX activation in NSCLC cells in response to gefitinib.

In addition, we show that the Areg-mediated inactivation of BAX in the cytosol is the consequence of the inhibition of Ku70 acetylation (Fig. 3). Accordingly, the knock down of Areg enhances gefitinib-induced Ku70 acetylation, leading to BAX release in its active, pro-

apoptotic form. This important result suggests that Areg could play pivotal regulatory functions by influencing the acetylation of intracellular proteins.

Acetylation is emerging as an important mechanism by which many non-histone proteins are regulated [23, 24]. Cell stress causes CBP- and/or PCAF-dependent Ku70 acetylation. In addition, we proved that HDAC inhibitors such as TSA can increase Ku70 acetylation. In both case, this acetylation of Ku70 is leading to the release of the pro-apoptotic form of BAX [14], which can translocate to the mitochondria, destabilize it and induce apoptosis [10, 17, 19, 22]. We also observed that overexpression of CBP or a TSA treatment in H358 cells sharply increased gefitinib-induced apoptosis. In our model, HDAC inhibitors such as TSA increased Ku70 acetylation and inhibited the BAX-Ku70 interaction, sensitizing H358 cells to gefitinib-induced apoptosis. These data demonstrated the involvement of both acetylases and deacetylases in Areg-dependent gefitinib-induced apoptosis regulation. These results also indicate that disruption of HAT-HDAC equilibrium governs non-histone protein acetylation such as Ku70, thereby affecting Areg-dependent gefitinib resistance.

Ku70 is targeted for deacetylation by both class I/II HDAC and class III/sirtuin deacetylases [10, 17, 25]. Accordingly, we observed an increased sensitivity to gefitinib under TSA, vorinostat and NAM treatments. Thus, classes I/II and class III/sirtuin deacetylases participate in the regulation of Areg-induced resistance to apoptosis by regulating Ku70 acetylation. Interestingly, class IIb HDAC is involved in lung carcinogenesis [26]. Further experiments are needed to clearly identify which HDAC can be involved in this mechanism.

Our results suggested that HDAC inhibitors counteract the protective effect of Areg and sensitize cells to gefitinib by increasing the level of acetylated Ku70, thus inducing the release of active BAX from Ku70. This key result encourages the use of HDAC inhibitors as anticancer agents [27]. Indeed, HDACs are involved in several human cancers [28]. HDAC

inhibitors were developed for cancer therapy and vorinostat was approved for treatment of cutaneous T cell lymphoma (CTCL) in 2006 [29]. Recently, the HDAC inhibitor romidepsin has been shown to enhance the antitumor effect of EGFR-TKI erlotinib in NSCLC cell lines [30]. We investigated an *in vivo* study combining HDAC inhibitors and EGFR-TKI on mice bearing NSCLC tumors. For the first time to our knowledge, a *per os* combination of vorinostat and gefitinib showed a major effect on inhibition of tumor growth. In tumors extracted 35 days after the beginning of treatment, vorinostat and gefitinib combined treatment induced an important and additive cell growth arrest. In addition, the cumulative effect of the dual treatment on apoptosis was obvious *in vitro* but was not significantly more elevated *in vivo*.

The sub-optimal doses of gefitinib and vorinostat, determined in preliminary experiments (not shown), are not associated with any documented side-effect, and no sign of toxicity was observed in the co-treated animals. Possible effect of vorinostat on the average level of protein acetylation in the tumor extracts after completion of the treatment was not detected by western blot or immunohistochemistry. This is in agreement with other studies, which also failed to establish a correlation between the acetylation status and the tumor response [31]. This result strongly supports the value of associating HDAC inhibitors and EGFR-TKI in NSCLC treatment, especially for EGFR-TKI-resistant patients. The molecular pathways activated *in vivo* by this combination of treatments, and especially the role of Ku70, still remain to be formally established.

In summary, our findings provide evidence that Areg mediates gefitinib resistance in NSCLC cells through an original acetylation-dependent pathway. Areg reduces Ku70 acetylation, therefore strengthening the functional inhibition of BAX. This results in the inhibition of gefitinib toxicity in NSCLC cells. The involvement of acetylation mechanisms in gefitinib

sensitivity should encourage the application of HDAC inhibitors as anticancer agents or in combination with EGFR-TKI treatments, especially in EGFR-TKI-resistant patients. Further studies are needed to validate whether the gefitinib treatment combined with HDAC inhibition could enhance the objective response and survival rates in NSCLC patients. Moreover, we demonstrated the therapeutic potential of Areg siRNAs combined with gefitinib treatment in NSCLC (see suppl. file S1). It could be interesting to combine a specific anti-Areg siRNAs treatment with gefitinib, in order to augment its therapeutic benefit (see suppl. file S1).

Materials and Methods

Cell Culture and drug treatments

The human H358 and H322 NSCLC cell lines were from the American Type Culture Collection (Manassas, VA) and maintained in RPMI 1640 medium (Gibco, Cergy Pontoise, France) supplemented with 10% heat-inactivated Fetal Bovine Serum (FBS) in a humidified atmosphere with 5% CO_2. Gefitinib was kindly provided by Astra-Zeneca France (Paris, France) and was prepared as 10 mM stock solution in DMSO and stored at -20°C. Recombinant human amphiregulin (Areg) was from Sigma-Aldrich (St Quentin Fallavier, France) and stored at -80°C in DMSO and dissolved in fresh medium just before use. Trichostatin A (TSA) was from Sigma-Aldrich and prepared as 25 µg/ml stock solution, nicotinamide (NAM) was from Sigma-Aldrich and prepared as 1 M stock solution, and suberoylanilide hydroxamic acid (SAHA, vorinostat) was from Indofine Chemical Soc,

(Hillsborough, USA), prepared as 10 mM stock solution and stored at -20°C. Cells were treated as indicated in figures legends.

Transfections

Small interfering RNAs (siRNAs) targeting human Areg, human Ku70 and non-specific control siRNAs were synthesized by MWG Biotech (Roissy, France). Sequences of siRNAs targeting Areg were 5'-CGA-ACC-ACA-AAU-ACC-UGG-CTT-3' and 5'-CCU-GGA-AGC-AGU-AAC-AUG-CTT-3'. Sequences of siRNAs targeting Ku70 were 5'-GAU-GCC-CUU-UAC-UGA-AAA-ATT-3' and 5'-UUC-UCU-UGG-UAA-CUU-UCC-CTT-3' and control siRNA sequence was 5'-CUU-ACG-CUC-ACU-ACU-GCG-ATT-3'. Transfection of duplex siRNAs was performed with Oligofectamine^{TM} reagent (Invitrogen, Cergy Pontoise, France), following the manufacturer's instructions. SiRNAs were transfected into 60% confluent cells at the final concentration of 200 nM. After transfection, the efficiency of Areg knockdown was assessed by ELISA as previously described [15] and the efficiency of Ku70 knockdown was assessed by western blotting.

Transient transfections were carried out on H358 cells cultured on Lab-Tek® two wells. Cells were transfected using Fugene (Roche Diagnostics, Meylan, France) according to the manufacturer's protocol, with 1.5 µg of an expression vector encoding CBP-HA or a control vector encoding green fluorescent protein (GFP). H358 cells were also transfected with control-pBJ5 or pBJ5-Ku70 wild-type (WT, provided by D. Trouche) or pBJ5-Ku70 K539R/K542R (generated using a QuickChange site-directed mutagenesis kit, Stratagene), along with pEGFP-C1 expression vector (Clontech), using JetPEI (PolyPlus Transfection) and according manufacturer's instructions. Immunofluorescence was performed 96h after transfection.

Apoptosis assays

Cells were harvested and pooled. The morphological changes related to apoptosis were assessed by fluorescence microscopy after Hoechst 33342 (5 µg/ml, Sigma) staining of cells and the percent of apoptotic cells was scored after counting at least 500 cells. Active caspase-3 was detected by flow cytometry using phycoerythrin-conjugated monoclonal active caspase-3 antibody kit (Becton Dickinson Pharmingen, Pont de Claix, France), following manufacturer's instructions. Analysis was performed on a Becton Dickinson FACScan flow cytometer with CellQuest Software (Becton Dickinson).

Protein immunostaining by flow cytometry

Activated BAX immunostaining analysis was performed as previously described [8, 32]. Briefly, fixed cells were first incubated with anti-activated BAX antibody (N-20, Santa Cruz Biotechnology, Tebu, 1:100) or with irrelevant IgG (Pharmingen, Becton Dickinson). Then washed cells were incubated with Alexa^{TM} 488 anti-rabbit IgG (H+L) conjugate (Interchim, 1:1000). Analysis was performed on a FACScan flow cytometer (Becton Dickinson) using Cellquest software. Green fluorescence was excited at 488 nm and detected at 500-550 nm.

Immunofluorescence staining

Cells cultured on Lab-Tek® were transfected as indicated. 96h after transfection, fixed cells were incubated with anti-HA.11 (Covance, Eurogentec, 1:1000). Second incubation was performed with Alexa^{TM} 488 goat anti-rabbit IgG (H+L) conjugate (Interchim, Montluçon, France, 1:500). Cells were then counterstained with Hoechst 33342 and observed using an Olympus microscope.

Subcellular fractionation and protein extraction

Total cell lysates were obtained after washing cells twice in PBS and incubated in RIPA lysis buffer (Tris-HCl 50 mM pH 7.4, NaCl 150 mM, Nonidet P-40 1%, sodium deoxycholate 0.5%, SDS 0.1%) with proteases and phosphatases inhibitors (NaF 1 mM, Na_3VO_4 1 mM, PMSF 0.5 mM, leupeptin 10 µg/ml, aprotinin 10 µg/ml and pepstatin 10 µg/ml) for 30 min on ice.

Cytosolic extracts for acetylation experiments were obtained as follow: cells were incubated with 50 ng/ml TSA overnight before 15 min. incubation in hypotonic buffer (100 ng/ml TSA, Tris-HCl pH 7.5 10mM, KCl 10mM, $MgCl_2$ 1.5mM, DTT 0.5 mM) with protease and phophatase inhibitors. Cells were then incubated 10 min. with hypotonic buffer supplemented with NP40 1%). The supernatant contained the cytoplasmic proteins.

Fractions extracts were assessed for protein content using the Bio-Rad D C Protein Assay kit, and 20 µg of proteins were subjected to electrophoresis and analyzed by western blotting for BAX and Ku70 content. The relative purity of fractions was ascertained by western blotting using α-tubulin (Sigma Aldrich) as a marker of cytosol and histone H3 (Upstate) as a marker of nucleus.

Immunoblotting and coimmunoprecipitation

Endogenous BAX immunoprecipitations were performed using 1 mg protein from whole-cell extracts and 1 µg BAX antibody (BD Pharmingen) or irrelevant rabbit IgG for negative control and by incubating overnight at 4°C under gentle agitation. Cytosolic Ku70 immunoprecipitations were done using 4 mg protein and 1 µg Ku70 antibody (Santa Cruz, Tebu-Bio) or irrelevant mouse IgG_{2b} for negative control and by incubating overnight at 4°C under agitation. The immunocomplexes were collected using protein-G agarose (Sigma-Aldrich). The immunoprecipitates were resolved on SDS-PAGE gels, followed by western

blotting with acetylated protein (Abcam, 1/1000), Ku70 (Santa Cruz, Tebu-Bio, 1/1000) or BAX (BD Pharmingen, 1/3000) antibodies. The immunoblot for acetylated protein was reprobed with Ku70 antibody to confirm the presence of an overlapping Ku70 band.

Western blotting was also done using anti-cleaved caspase-3 (Asp 175, Cell Signaling, 1/1000) antibodies. To ensure equal loading and transfer, membranes were also probed for actin using anti-actin antibody (Sigma, 1/1000). Western blotting was further processed by standard procedures and revealed by chemiluminescence (ECL, Amersham, Orsay, France).

The relative intensity, measured using ImageJ (NIH software), of acetylated Ku70 bands or total Ku70 of treated samples to that of control cells was normalized to the respective Ku70 or BAX, respectively.

***In vivo* model**

The effect of the combination of gefitinib and vorinostat was measured on established subcutaneous tumor bearing mice. All the animal experiments were performed in agreement with the EEC guidelines and the "Principles of laboratory animal care" (NIH publication N°86-23 revised 1985). The experimental protocol was submitted to ethical evaluation and the experiment received the accreditation number was #0260. Human lung adenocarcinoma H358 cells were harvested from culture, and $20x10^6$ cells in sterile PBS were injected subcutaneously into the flank of female NMRI *nude* mice (6-8 weeks old, Janvier, Le Genest Saint Isle, France). When tumor diameters reached 5 mm, mice were randomised in four experimental groups (10 mice/group). Group 1 (control mice) received a vehicle (tween/glucose), group 2 received vorinostat, group 3 received gefitinib, and group 4 received both vorinostat and gefitinib. Five mg/kg/day of gefitinib and/or 100 mg/kg/day of vorinostat were administered *per os* in tween/glucose, 5 days a week. Tumor growth was quantified by measuring twice a week the tumors in two dimensions with a Vernier caliper. The volume

was calculated as follow: a x b^2 x 0.4, where a and b are the largest and smallest diameters respectively. Results are expressed as volume ± S.E.M. Mice bearing necrotic tumors or tumors ≥ 1.5 cm in diameter were euthanized immediately. On day 36, all mice were sacrificed and tumors were collected before further analyses by western blotting and immunohistochemistry.

Immunohistochemical staining

Tumor sections of 7 µm thickness were fixed with 3.7% paraformaldehyde for 10 min at room temperature, then saturated for 5 min with 0.03% BSA, incubated overnight at 4°C with rabbit anti-acetylated lysine antibody (Cell signaling, 1/200) or with monoclonal mouse anti-human Ki67 (DAKO, 1/150). Immunohistochemistry was further processed using the Histostain-Plus Bulk Kit (Invitrogen). The final reaction product was visualized with diaminobenzidine. After immunohistochemical reactions, sections were counterstained with hematoxylin. Negative controls were performed with the same sections incubated with irrelevant antibody (rabbit IgG 1/40000 or mouse IgG 1/30000).

Statistical analyses

Statistical significance of difference in treatment was analyzed by Mann Whitney test. Means comparisons among groups and statistical significance of differences in tumor growth in the combination treatment group and in single-agent treatment groups were analyzed by ANOVA test. Statistics were done using Statview 4.1 software (Abacus Concept Inc.). In all statistical analyses, two-sided *p* values < 0.05 were considered statistically significant.

Acknowledgments

We thank AstraZeneca for gefitinib, D. Trouche (CNRS UMR5088, France) for Ku70 wild-type expression vector, Laetitia VanWonterghem and Corine Tenaud for technical assistance. This work was supported by grants and research fellowship from La Ligue contre le Cancer, comité de la Drôme; EpiPro program (InCa) and "projet libre INCa", PL06_025, to MCF and SK laboratories; ARECA program (ARC) to SK laboratory and with the help of a "subvention-libre" from the ARC (Association pour la Recherche sur le Cancer).

References

1. Garcia de Palazzo, IE, Adams, GP, Sundareshan, P, Wong, AJ, Testa, JR, Bigner, DD, *et al.* (1993). Expression of mutated epidermal growth factor receptor by non-small cell lung carcinomas. *Cancer Res* **53**: 3217-3220.
2. Rusch, V, Baselga, J, Cordon-Cardo, C, Orazem, J, Zaman, M, Hoda, S, *et al.* (1993). Differential expression of the epidermal growth factor receptor and its ligands in primary non-small cell lung cancers and adjacent benign lung. *Cancer Res* **53**: 2379-2385.
3. Fukuoka, M, Yano, S, Giaccone, G, Tamura, T, Nakagawa, K, Douillard, JY, *et al.* (2003). Multi-institutional randomized phase II trial of gefitinib for previously treated patients with advanced non-small-cell lung cancer (The IDEAL 1 Trial) [corrected]. *J Clin Oncol* **21**: 2237-2246.

4. Shepherd, FA, Rodrigues Pereira, J, Ciuleanu, T, Tan, EH, Hirsh, V, Thongprasert, S, *et al.* (2005). Erlotinib in previously treated non-small-cell lung cancer. *N Engl J Med* **353**: 123-132.

5. Thatcher, N, Chang, A, Parikh, P, Rodrigues Pereira, J, Ciuleanu, T, von Pawel, J, *et al.* (2005). Gefitinib plus best supportive care in previously treated patients with refractory advanced non-small-cell lung cancer: results from a randomised, placebo-controlled, multicentre study (Iressa Survival Evaluation in Lung Cancer). *Lancet* **366**: 1527-1537.

6. Ishikawa, N, Daigo, Y, Takano, A, Taniwaki, M, Kato, T, Hayama, S, *et al.* (2005). Increases of amphiregulin and transforming growth factor-alpha in serum as predictors of poor response to gefitinib among patients with advanced non-small cell lung cancers. *Cancer Res* **65**: 9176-9184.

7. Busser, B, Coll, JL, and Hurbin, A (2008). The increasing role of amphiregulin in non-small cell lung cancer. *Pathol Biol (Paris).*

8. Hurbin, A, Coll, JL, Dubrez-Daloz, L, Mari, B, Auberger, P, Brambilla, C, *et al.* (2005). Cooperation of amphiregulin and insulin-like growth factor-1 inhibits Bax- and Bad-mediated apoptosis via a protein kinase C-dependent pathway in non-small cell lung cancer cells. *J Biol Chem* **280**: 19757-19767.

9. Scorrano, L, and Korsmeyer, SJ (2003). Mechanisms of cytochrome c release by proapoptotic BCL-2 family members. *Biochem Biophys Res Commun* **304**: 437-444.

10. Cohen, HY, Lavu, S, Bitterman, KJ, Hekking, B, Imahiyerobo, TA, Miller, C, *et al.* (2004). Acetylation of the C terminus of Ku70 by CBP and PCAF controls Bax-mediated apoptosis. *Mol Cell* **13**: 627-638.

11. Gullo, C, Au, M, Feng, G, and Teoh, G (2006). The biology of Ku and its potential oncogenic role in cancer. *Biochim Biophys Acta* **1765**: 223-234.

12. Featherstone, C, and Jackson, SP (1999). Ku, a DNA repair protein with multiple cellular functions? *Mutat Res* **434**: 3-15.

13. Tuteja, R, and Tuteja, N (2000). Ku autoantigen: a multifunctional DNA-binding protein. *Crit Rev Biochem Mol Biol* **35**: 1-33.

14. Witta, SE, Gemmill, RM, Hirsch, FR, Coldren, CD, Hedman, K, Ravdel, L, *et al.* (2006). Restoring E-cadherin expression increases sensitivity to epidermal growth factor receptor inhibitors in lung cancer cell lines. *Cancer Res* **66**: 944-950.

15. Hurbin, A, Dubrez, L, Coll, JL, and Favrot, MC (2002). Inhibition of apoptosis by amphiregulin via an insulin-like growth factor-1 receptor-dependent pathway in non-small cell lung cancer cell lines. *J Biol Chem* **277**: 49127-49133.

16. Desagher, S, Osen-Sand, A, Nichols, A, Eskes, R, Montessuit, S, Lauper, S, *et al.* (1999). Bid-induced conformational change of Bax is responsible for mitochondrial cytochrome c release during apoptosis. *J Cell Biol* **144**: 891-901.

17. Subramanian, C, Opipari, AW, Jr., Bian, X, Castle, VP, and Kwok, RP (2005). Ku70 acetylation mediates neuroblastoma cell death induced by histone deacetylase inhibitors. *Proc Natl Acad Sci U S A* **102**: 4842-4847.

18. Subramanian, C, Jarzembowski, JA, Opipari, AW, Jr., Castle, VP, and Kwok, RP (2007). CREB-binding protein is a mediator of neuroblastoma cell death induced by the histone deacetylase inhibitor trichostatin A. *Neoplasia* **9**: 495-503.

19. Sutheesophon, K, Kobayashi, Y, Takatoku, MA, Ozawa, K, Kano, Y, Ishii, H, *et al.* (2006). Histone deacetylase inhibitor depsipeptide (FK228) induces apoptosis in leukemic cells by facilitating mitochondrial translocation of Bax, which is enhanced by the proteasome inhibitor bortezomib. *Acta Haematol* **115**: 78-90.

20. Mazumder, S, Plesca, D, Kinter, M, and Almasan, A (2007). Interaction of a cyclin E fragment with Ku70 regulates Bax-mediated apoptosis. *Mol Cell Biol* **27**: 3511-3520.

21. Ju, DS, Kim, MJ, Bae, JH, Song, HS, Chung, BS, Lee, MK, *et al.* (2007). Camptothecin acts synergistically with imatinib and overcomes imatinib resistance through Bcr-Abl independence in human K562 cells. *Cancer Lett* **252**: 75-85.

22. Lee, SM, Bae, JH, Kim, MJ, Lee, HS, Lee, MK, Chung, BS, *et al.* (2007). Bcr-Abl-independent imatinib-resistant K562 cells show aberrant protein acetylation and increased sensitivity to histone deacetylase inhibitors. *J Pharmacol Exp Ther* **322**: 1084-1092.

23. Spange, S, Wagner, T, Heinzel, T, and Kramer, OH (2009). Acetylation of non-histone proteins modulates cellular signalling at multiple levels. *Int J Biochem Cell Biol* **41**: 185-198.

24. Minucci, S, and Pelicci, PG (2006). Histone deacetylase inhibitors and the promise of epigenetic (and more) treatments for cancer. *Nat Rev Cancer* **6**: 38-51.

25. Sundaresan, NR, Samant, SA, Pillai, VB, Rajamohan, SB, and Gupta, MP (2008). SIRT3 is a stress-responsive deacetylase in cardiomyocytes that protects cells from stress-mediated cell death by deacetylation of Ku70. *Mol Cell Biol* **28**: 6384-6401.

26. Kamemura, K, Ito, A, Shimazu, T, Matsuyama, A, Maeda, S, Yao, TP, *et al.* (2008). Effects of downregulated HDAC6 expression on the proliferation of lung cancer cells. *Biochem Biophys Res Commun* **374**: 84-89.

27. Bolden, JE, Peart, MJ, and Johnstone, RW (2006). Anticancer activities of histone deacetylase inhibitors. *Nat Rev Drug Discov* **5**: 769-784.

28. Yang, XJ, and Seto, E (2007). HATs and HDACs: from structure, function and regulation to novel strategies for therapy and prevention. *Oncogene* **26**: 5310-5318.

29. Grant, S, Easley, C, and Kirkpatrick, P (2007). Vorinostat. *Nat Rev Drug Discov* **6**: 21-22.

30. Zhang, W, Peyton, M, Xie, Y, Soh, J, Minna, JD, Gazdar, AF, *et al.* (2009). Histone deacetylase inhibitor romidepsin enhances anti-tumor effect of erlotinib in non-small cell lung cancer (NSCLC) cell lines. *J Thorac Oncol* **4**: 161-166.

31. Prince, HM, Bishton, MJ, and Harrison, SJ (2009). Clinical studies of histone deacetylase inhibitors. *Clin Cancer Res* **15**: 3958-3969.

32. Dubrez, L, Coll, JL, Hurbin, A, Solary, E, and Favrot, MC (2001). Caffeine sensitizes human H358 cell line to p53-mediated apoptosis by inducing mitochondrial translocation and conformational change of BAX protein. *J Biol Chem* **276**: 38980-38987.

Figures legends

Figure 1. Areg and Ku70 inhibit gefitinib-induced apoptosis.

H358 cells were transfected with control or Areg or Ku70 siRNAs and treated with 0.5 µM gefitinib. (a) The efficiency of Areg knock down was assessed by ELISA. Results are expressed as a rate of Areg released 48 h to 96 h after control siRNAs transfection and as mean ± SD (n=3). (b) The efficiency of Ku70 knock down was assessed after 96 h by western-blotting using Ku70 antibody. (c) Apoptosis was scored after counting Hoechst stained cells. Results are expressed as mean ± SD (n≥3). * $p<0.05$, *** $p<0.001$, for comparison between treated and control cells.

Figure 2. Areg and Ku70 inactivate BAX in H358 cells.

H358 cells were transfected with control or Areg or Ku70 siRNAs and/or treated with 0.5 µM gefitinib. (a) Flow cytometry analysis of BAX immunostaining using activated-BAX antibody. Dotted histogram, irrelevant antibody; open histogram, control cells; filled histogram, treated cells as indicated. (b) Percentages of activated BAX stained cells were expressed as mean ± SD (n≥3). * $p<0.05$, more significant than control.

Figure 3. Areg enhances BAX-Ku70 interaction and inhibits Ku70 acetylation.

H358 cells were transfected with control or Areg siRNAs and 0.5 µM gefitinib was applied as indicated for 96 h (a, c). H322 cells were treated or not (NT) with 50 ng/ml Areg and 0.5 µM gefitinib for 96 h as indicated (b). (a, b) Endogenous BAX immunoprecipitation (IP) was performed from whole-cell extracts and subjected to immunoblotting with Ku70 and BAX antibodies. The values denote the relative intensity of Ku70 protein bands of treated samples

to that of control cells, after being normalized to the respective BAX and represent the average ± SD of independent experiments (H358 n=3; H322 n=2). (c) Endogenous Ku70 IP was performed from cytosolic extracts and subjected to immunoblotting with anti-acetylated proteins and BAX antibodies. The immunoblot was reprobed with Ku70 antibody to confirm the presence of an overlapping Ku70 band. The values denote the relative intensity of acetylated Ku70 bands of treated samples to that of control cells, after being normalized to the respective Ku70 and represent the average ± SD of 3 independent experiments. Cytoplasmic α-tubulin and nuclear histone H3 were used to show that cytoplasmic extracts were nuclear-free. IgG: irrelevant immunoglobulins, used as negative control. Inputs: cell lysates not subjected to immunoprecipitation.

Figure 4. Enhanced Ku70 acetylation sensitizes H358 cells to gefitinib.

(a) H358 cells were transfected with a plasmid control encoding GFP or with a plasmid encoding CBP-HA and treated or not (NT) with 0.5 µM gefitinib as indicated. The expression of GFP or CBP-HA was revealed by immunofluorescence 96 h after transfection and apoptosis of transfected cells was analyzed after counting Hoechst-stained cells. (b-d) H358 cells were treated or not (NT) with TSA (b), vorinostat (c), nicotinamide (d, NAM) and/or 0.5 µM gefitinib. Apoptosis was scored after counting Hoechst-stained cells. Results are expressed as mean ± SD (n≥3). * $p<0.05$, *** $p<0.001$, more significant than control.

Figure 5. TSA-induced Ku70 acetylation regulates gefitinib-mediated apoptosis.

(a) H358 cells were treated with 0.5 µM gefitinib and/or 200 ng/ml TSA. Endogenous Ku70 immunoprecipitation (upper panel) was performed from cytosolic extracts and subjected to immunoblotting with anti-acetylated proteins antibody. The immunoblot was reprobed with Ku70 antibody to confirm the presence of an overlapping Ku70 band. Endogenous BAX

immunoprecipitation (middle panel) was performed from whole-cell extracts and subjected to immunoblotting with Ku70 and BAX antibodies. The values denote the relative intensity of Ku70 protein bands of treated samples to that of control cells, after being normalized to the respective BAX and represent the average ± SD of three independent experiments. Cytoplasmic α-tubulin and nuclear histone H3 were used to show that cytoplasmic extracts were nuclear-free (lower panel). IgG: irrelevant immunoglobulins. Inputs: cell lysates not subjected to immunoprecipitation. (b) H358 cells were co-transfected with pEGFP-C1 and with control-pBJ5 or pBJ5-Ku70 wild-type (WT) or pBJ5-Ku70 K539R/K542R expression plasmids. Gefitinib 0.5 μM and/or TSA 200 ng/ml were added for 96 h. Apoptosis was determined after Hoechst staining and counting apoptotic cells per 100 GFP-positive cells. Results are expressed as mean ± SD (n=3). *, $p<0.05$, less significant than control.

Figure 6. Antitumoral activity of gefitinib and HDAC inhibitor combined treatment *in vivo*

(a) Effects of combined treatment with gefitinib and vorinostat on growth of H358 xenograft tumors in athymic nude mice. The mice were randomly assigned to one of four treatment groups. Group 1 (control mice) received vehicle, group 2 received gefitinib, group 3 received vorinostat, and group 4 received gefitinib and vorinostat. Gefitinib (5 mg/kg body weight) or vorinostat (100 mg/kg body weight) were administered p.o. 5 days/week. Tumor volumes were measured 3 times a week. Points, mean tumor volume (n = 8); bars, SE. *, $p<0.05$, **, $p<0.01$, for comparisons between treated and control for each serie of experiments. (b) Acetylated proteins and Ki67 nuclear protein detected by immunostaining on frozen tumor sections from control mice, mice treated with vorinostat, gefitinib or both gefitinib and vorinostat, as indicated. IgG, irrelevant antibody. Scale bars correspond to 50 μm. Histogram: the percentage of positive cells for Ki67 was determined after counting stained cells per 1000

cells on a section. Results are expressed as mean ± SD (n=6 mice per group); **, p=0.0039 for comparisons between combined treatment and control or single treatment. (c) Effect of gefitinib and vorinostat on the expression of activated-caspase-3 in H358 xenograft tumors, assessed by western blotting. Actin was used as loading control.

Table 1. Synergistic indexes of combination treatment of gefitinib and vorinostat

Drug	Control	Vorinostat (treatment A)	Gefitinib (treatment B)	Vorinostat + gefitinib		
Mean volume (mm^3 ± SE)	1442 ± 513	1262 ± 786	1454 ± 869	524 ± 243		
Mean Growth Inhibition[1]	1	0.88	1.01	0.89[2]	0.36[3]	2.47[4]
P value[5]	-	0.468	0.663	0.0029		

Growth inhibition rate on established subcutaneous tumor nodules in athymic nude mice treated with indicated concentrations of vorinostat, gefitinib or their combinations. [1]Mean growth inhibition rate (MGI) = growth rate of treated group/growth rate of untreated group. [2]Expected MGI: growth inhibition rate of treatment A x growth inhibition rate of treatment B. [3]Observed MGI: growth inhibition rate of combined treatment on treatments A and B. [4]Index: calculated by dividing the expected growth inhibition rate by the observed growth inhibition rate. An index over 1 indicates synergistic effect and less than 1 indicates less than additive effect. [5]*P* value was calculated by *t* test compared to control treatment.

Figure 1

Click here to download high resolution image

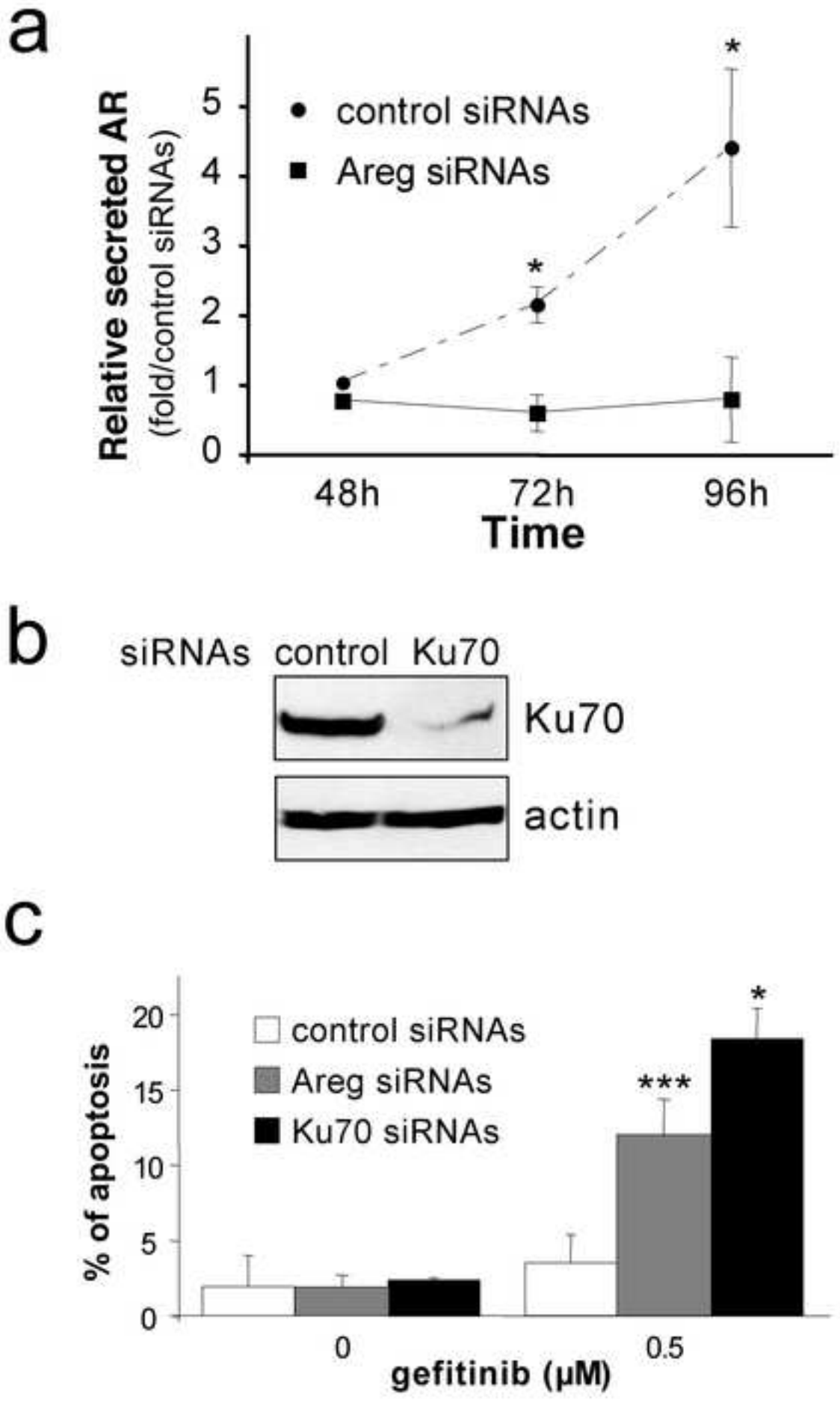

Figure 2

Click here to download high resolution image

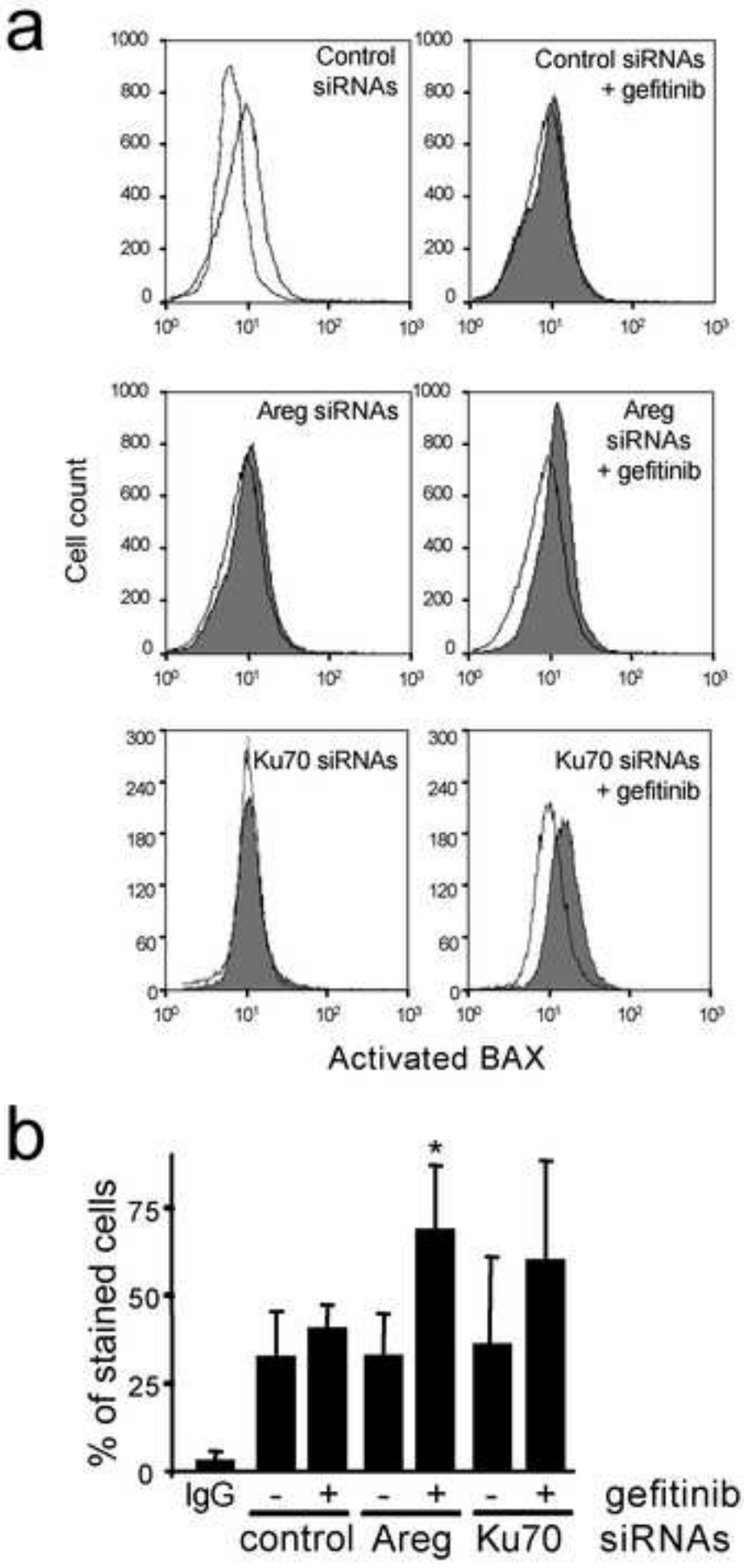

Figure 3

Click here to download high resolution image

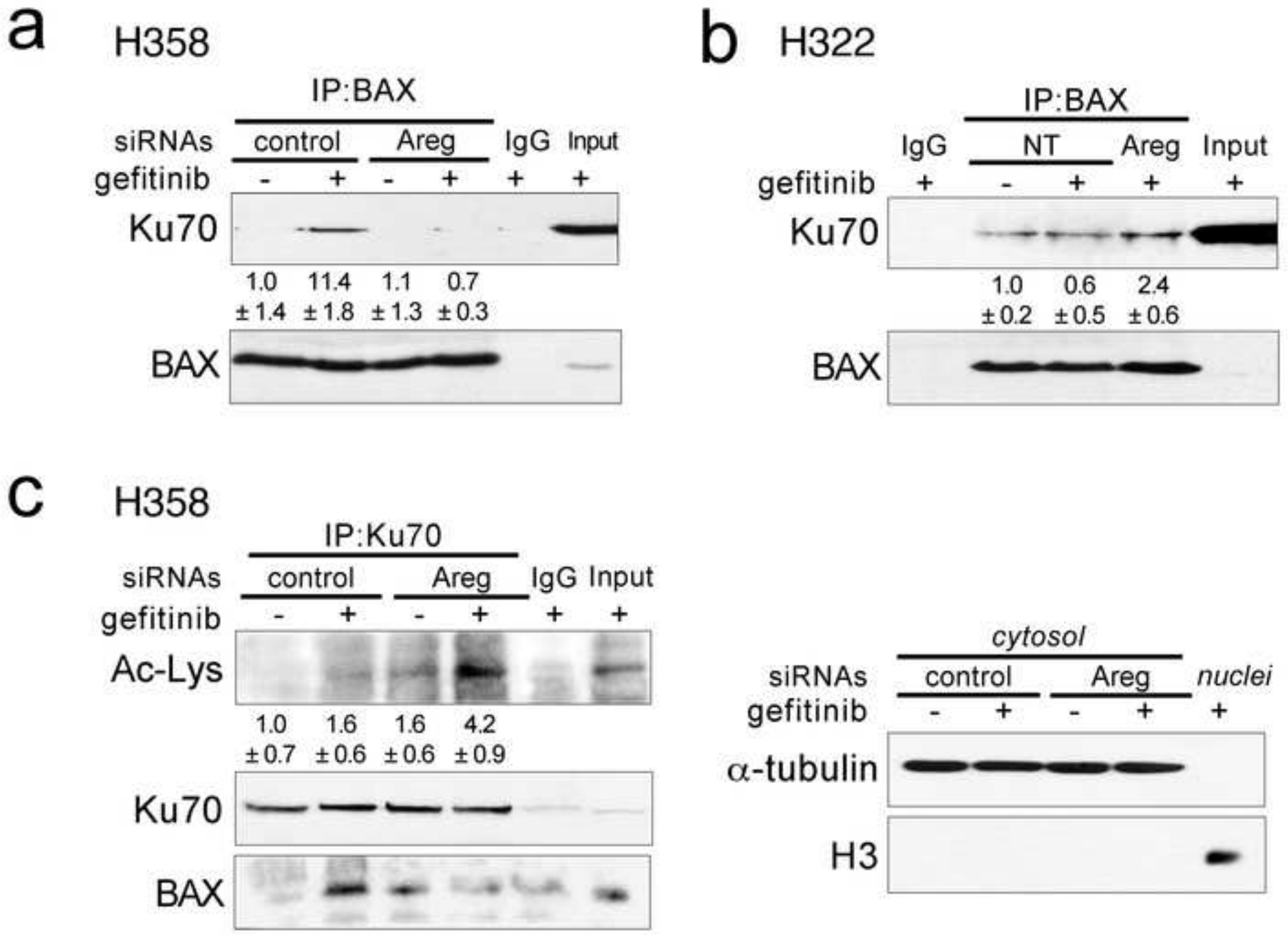

Figure 4

Click here to download high resolution image

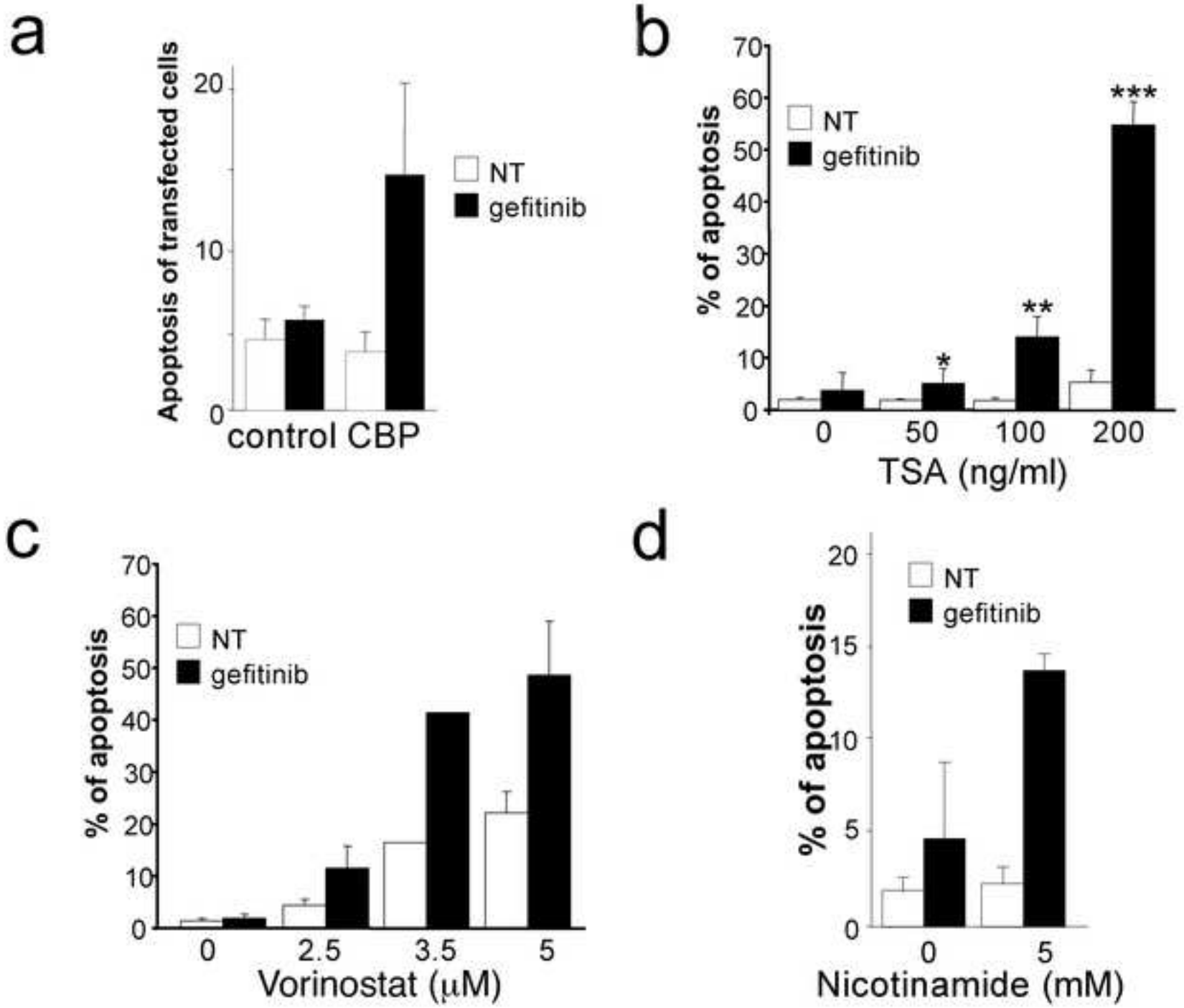

Figure 5

Click here to download high resolution image

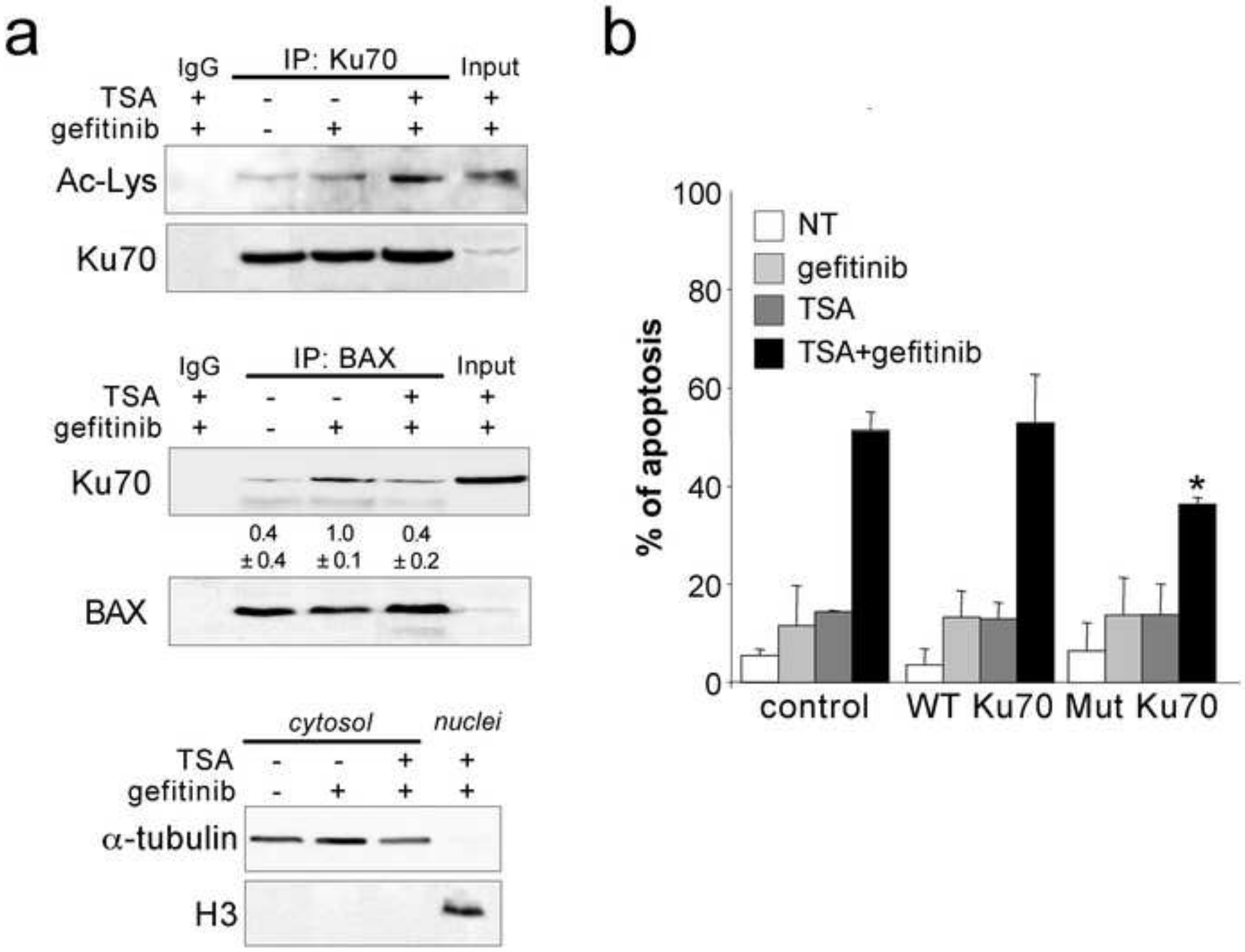

Figure 6

Click here to download high resolution image